

Analytical Solution and Satellite Phasing Rules for Designing Dedicated Geosynchronous Orbit Satellite Constellations

Soung Sub Lee

Department of Aerospace System Engineering, Sejong University, 209, Neungdong-Ro, Gwangjin-Gu, Seoul, 05006, South Korea.

Correspondence

SS Lee
Department of Aerospace System Engineering, Sejong University, 209, Neungdong-Ro, Gwangjin-Gu, Seoul, 05006, South Korea.
Email: spacein0320@gmail.com

Abstract

This study proposes a dedicated closed-form solution and satellite phasing rules for designing a geosynchronous orbit (GSO) constellation. Trajectories of GSO satellites have a characteristic figure-eight shape because their rotation speed is the same as that of the Earth. The GSO has the advantage of providing good coverage performance for local areas. Recently, several countries have begun developing local navigation systems based on the GSO. Various GSO constellation designs are available for an effective regional navigation performance analysis; however, no dedicated GSO constellation solution exists. This study provides a solution for such constellations and proves its practicability through a comparative analysis and evaluation of the geometric dilution-of-precision performance for several cases.

Keywords

closed-form solution; geometric dilution of precision; geosynchronous orbit constellation; regional performance; satellite phasing rules

1 | INTRODUCTION

Global navigation satellite systems (GNSSs) provide three-dimensional position and time synchronization information through distance measurements using satellite positions and radio waves received from a constellation of satellites in the Earth's orbit. Examples of GNSS technology include the United States' Global Positioning System (GPS), the Global Orbiting Navigation System (GLONASS) in Russia, Galileo in Europe, and the BeiDou Navigation Satellite System (BDS) in China.

The United States' GPS requires a minimum of 24 satellites, with 4 satellites per orbital plane in 6 medium Earth orbit (MEO) orbital planes. In total, 31 of the 35 satellites are functional (Kim, 2019). There are three generations of GPS satellites in operation, with 29 second-generation and 2 third-generation satellites currently in operation. The GPS continues to be modernized and developed, with new technologies and functions added for improved performance. GLONASS, Russia's satellite-based radio navigation system, was equipped with 24 satellites in 2014. As of September 2020, a constellation of 27 satellites (all in MEO) is in operation,

of which 23 are in normal operation, 1 is a backup, 1 is a test satellite, and 2 are in maintenance (Karutin, 2020). Although the modernization of GLONASS took approximately 20 years longer than that of the GPS, efforts to improve its performance have produced significant results. The development and construction of the European Galileo system began in 1999 as an independent GNSS that provides a variety of services for civilian use, unlike the GPS, which was developed for military use (Bandemer et al., 2006). The satellite constellation is in MEO, with an inclination angle of 56° . Overall, 28 satellites have been launched to date, of which 24 are operational, 2 are defunct, and 2 are unserviceable. China initially started its global satellite navigation program with BeiDou-1, a regional navigation system. In the intermediate stage, the country launched 35 satellites, which follow a combination of geostationary orbit (GEO) and MEO trajectories, and achieved its full operational capability with the BDS. The BDS consists of 3 GEO, 3 geosynchronous orbit (GSO), and 24 MEO satellites and provides various services in addition to satellite navigation services (Shen, 2020).

The four GNSSs described above independently provide location, speed, and time services globally, which enable the provision of global satellite navigation services by combining an MEO satellite constellation with the regional coverage characteristics of the GEO and GSO. GNSSs are primarily being developed in advanced spacefaring nations. These countries are accelerating the development and operation of their own satellite navigation systems in cases of emergency or for supplementing the GPS. Examples include the Navigation with Indian Constellation (NavIC) in India, the Quasi-Zenith Satellite System (QZSS) in Japan, and the Korean Positioning System (KPS) in South Korea.

India's NavIC is a regional satellite navigation system developed to break away from dependence on the United States' GPS. NavIC consists of seven satellites, including three GEO and four GSO satellites. Currently, NavIC plans to launch four additional satellites to expand its service coverage and provide precision and continuity with at least six satellites (Mukesh et al., 2020; Noer et al., 2020). Japan's QZSS is a system built to supplement the GPS. The QZSS consists of seven satellites, including three GEO and four GSO satellites (Ye et al., 2020; JAXA QZSS Project Team, 2009). Finally, the KPS is a system being planned in South Korea that will provide satellite navigation and various services to the East Asian region, including the Korean Peninsula. The satellite constellation will consist of three GEO and five GSO satellites (Shin et al., 2019).

The NavIC, QZSS, and KPS are regional satellite navigation systems that seek to achieve local full-coverage performance by combining the GEO and figure-eight-shaped GSO, with the trajectories fixed above the respective country. This study focuses solely on the GSO. The performance index of a regional satellite navigation system is an important factor for the constellation geometry of a GSO satellite group, as it can be used to improve the re-visit period and location accuracy. In general, the geometric dilution of precision (GDOP) is typically used to evaluate this performance index. The key issues for improving GDOP performance are visibility and coverage between satellites and ground targets, which have recently been studied in depth through a two-dimensional coverage analysis method with consideration of various constraints (Bai et al., 2024; Gu et al., 2024). Additionally, to evaluate the GDOP performance of a satellite group, a simple analytical solution is required to first design and compare various GSO constellation types. However, the literature does not provide a dedicated analytical solution that can be used to design and evaluate various GSO constellation structures.

This study makes three academic contributions. First, it provides a dedicated analysis tool consisting of phasing rules and a closed-form solution for designing various GSO satellite constellations. Second, this work compares and evaluates the performance of identical/non-identical patterns, equally/non-equally spaced placements, and circular/noncircular patterns for a GSO constellation. Third, the resulting solution serves as a tool for mission engineers to evaluate various GSO patterns, effectively design space missions, and improve regional GNSS performance by analyzing the geometric deployment characteristics. The remainder of this paper is organized as follows. Section 2 obtains a dedicated GSO solution from a mathematical model that describes the relative motion of two objects. Section 3 presents the phasing rule, where satellite constellations have the same ground track. Section 4 explains the GDOP, which is applied for evaluating the performance of the simulation results in Section 5.

2 | MATHEMATICAL MODELING

In this section, we derive a dedicated analytical solution for GSO designs in an Earth-centered, Earth-fixed (ECEF) coordinate system. Lee and Hall presented a comprehensive solution for the relative motion of satellites through parametric constellations (PCs) (Lee & Hall, 2021). As depicted in Figure 1, the relative motions are designed as hypocycloids, epicycloids, or their transformed parametric curves based on the correlation between the deferent circle and epicycle. Hypocycloid curves were drawn with the epicycle rolling inside the deferent circles, and epicycloid curves were drawn with the epicycle circle rolling outside.

We define a notation to describe the equations of motion for the relative motion of the satellites. In this study, “c” indicates the chief satellite, “d” denotes the deputy satellite, and the six orbital elements representing their motion are denoted by the general notations $[a, e, i, \Omega, \omega, M_0]$. The true anomaly, which is a function of

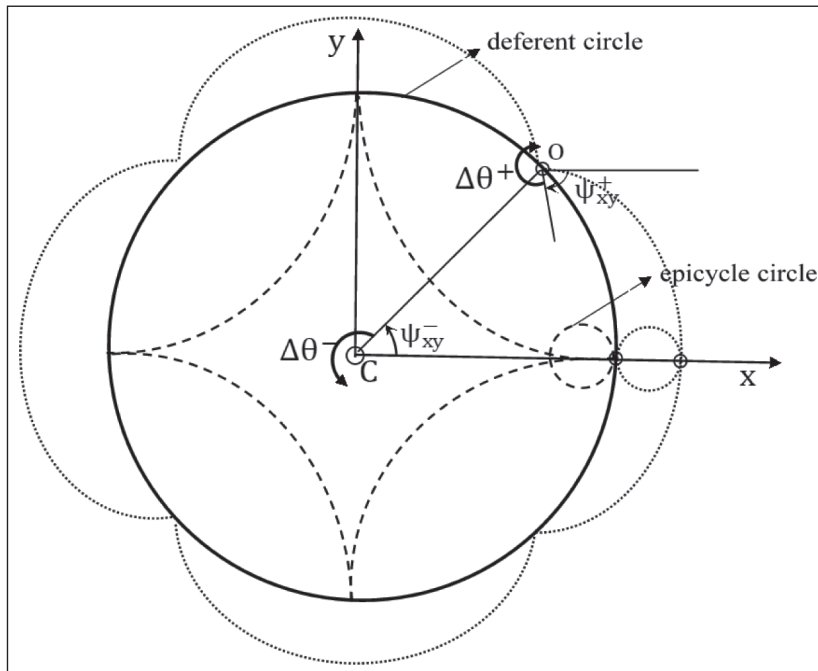


FIGURE 1 Hypocycloid and epicycloid curves by deferent circle and epicycle

time, is denoted by v , and the orbital radius is denoted by r . The PC theory does not consider perturbations, and the coordinate system represents the relative positions x, y, z of the deputy satellite with respect to the rotating reference frame of the chief satellite using the following generalized equations of motion:

$$x = \frac{r_d}{2} \left[(1 + \cos i_R) \cos(\Delta\theta^- + \psi_{xy}^-) + (1 - \cos i_R) \cos(\Delta\theta^+ + \psi_{xy}^+) \right] - r_c \quad (1a)$$

$$y = \frac{r_d}{2} \left[(1 + \cos i_R) \sin(\Delta\theta^- + \psi_{xy}^-) - (1 - \cos i_R) \sin(\Delta\theta^+ + \psi_{xy}^+) \right] \quad (1b)$$

$$z = r_d \sin i_R \sin(v_d + \psi_z) \quad (1c)$$

where the terms of the angular frequency $\Delta\theta^-$, $\Delta\theta^+$ and the phase angles ψ_{xy}^- , ψ_{xy}^+ , ψ_z , as well as ϕ_c and ϕ_d , are given as follows:

$$\Delta\theta^- = v_d - v_c \quad (2a)$$

$$\Delta\theta^+ = v_d + v_c \quad (2b)$$

$$\psi_{xy}^- = (\omega_d - \omega_c) - (\phi_d - \phi_c) \quad (2c)$$

$$\psi_{xy}^+ = (\omega_d + \omega_c) - (\phi_d + \phi_c) \quad (2d)$$

$$\psi_z = \omega_d - \phi_d \quad (2e)$$

$$\phi_c = \tan^{-1} \frac{(\sin \Delta\Omega \sin i_c \sin i_d)}{(-\cos i_d + \cos i_c \cos i_R)} \quad (3a)$$

$$\phi_d = \tan^{-1} \frac{(\sin \Delta\Omega \sin i_c \sin i_d)}{(\cos i_c - \cos i_d \cos i_R)} \quad (3b)$$

Here, i_R is the relative inclination between two satellites:

$$\cos i_R = \cos i_c \cos i_d + \sin i_c \sin i_d \cos \Delta\Omega \quad (4)$$

The relative ascending node $\Delta\Omega$ is defined as follows:

$$\Delta\Omega = \Omega_d - \Omega_c \quad (5)$$

The purpose of this study was to obtain a closed-form solution for designing a GSO from the equations of relative motion described above. The resulting solution represents the relative position of the GSO satellite with respect to a coordinate system in the International Terrestrial Reference Frame (ITRF). For this purpose, the parameters in Equations (2)–(4) were simplified as shown in Table 1.

TABLE 1
Parameters for GSO

Full equation of motion	For GSO
$\Delta\theta^-, \Delta\theta^+$	$v \mp (\omega_{\oplus} - \dot{\Omega})t$
ψ_{xy}^-, ψ_{xy}^+	$\omega \pm \Omega$
ψ_z	ω
ϕ_c, ϕ_d	0
i_R	i

The angular frequency terms in Table 1 vary as functions of the true anomaly of the satellite orbit and the rotational velocity of the Earth. The nodal drift $\dot{\Omega}$ is as follows (Kuiack & Ulrich, 2018):

$$\dot{\Omega} = -\frac{3}{2} J_2 n \frac{R_e^2}{p^2} \cos i \quad (6)$$

where R_e is the Earth's radius, J_2 is the oblateness perturbation, n is the mean motion of the satellite orbit, and $p = a(1 - e^2)$. The phase angle terms ψ_{xy}^-, ψ_{xy}^+ are also simplified as functions of ω and Ω of the satellite orbit. Consequently, by substituting the simplified parameters listed in Table 1 in Equation (1), we obtain a closed-form solution for computing the coordinates in the ITRF, a non-inertial frame of reference with its origin at the Earth's center of mass:

$$x = \frac{r}{2} \left[(1 + \cos i) \cos(v - (\omega_{\oplus} - \dot{\Omega})t + \omega + \Omega) + (1 - \cos i) \cos(v + (\omega_{\oplus} - \dot{\Omega})t + \omega - \Omega) \right] \quad (7a)$$

$$y = \frac{r}{2} \left[(1 + \cos i) \sin(v - (\omega_{\oplus} - \dot{\Omega})t + \omega + \Omega) - (1 - \cos i) \sin(v + (\omega_{\oplus} - \dot{\Omega})t + \omega - \Omega) \right] \quad (7b)$$

$$z = r \sin i \sin(v + \omega) \quad (7c)$$

As shown in Equation (7), the phase angle terms of the orbit are determined solely by ω and Ω , which will play important roles in the design of the GSO constellation in the next section. Moreover, Equation (7) is generally used to design the orbits of satellites rotating around Earth. To design the trajectory of the target GSO satellite, only the semi-major axis of the GSO (42,164.17 km) must be considered (Sjoberg et al., 2017).

Figure 2 depicts the orbit of a satellite near the GSO. Figure 2(a) shows the trajectory for a semi-major axis of 41,000 km and an inclination angle of 30°, where the values of the other orbital elements are all zero. The trajectory of the satellite follows a hypocycloid motion, and a loop is formed as it traces outward. In Figure 2(b), with a semi-major axis of 43,000 km, a loop forming inward can be observed, along with an epicycloid motion. In general, the loops are caused by the dynamics of the relative motion between Earth and the satellite, and the shape and number of loops are determined by the rotation rate between the two objects. Additionally, the trajectory featured in Figure 2 has a shape that differs from a figure-eight, owing to the difference in rotation rates between Earth and

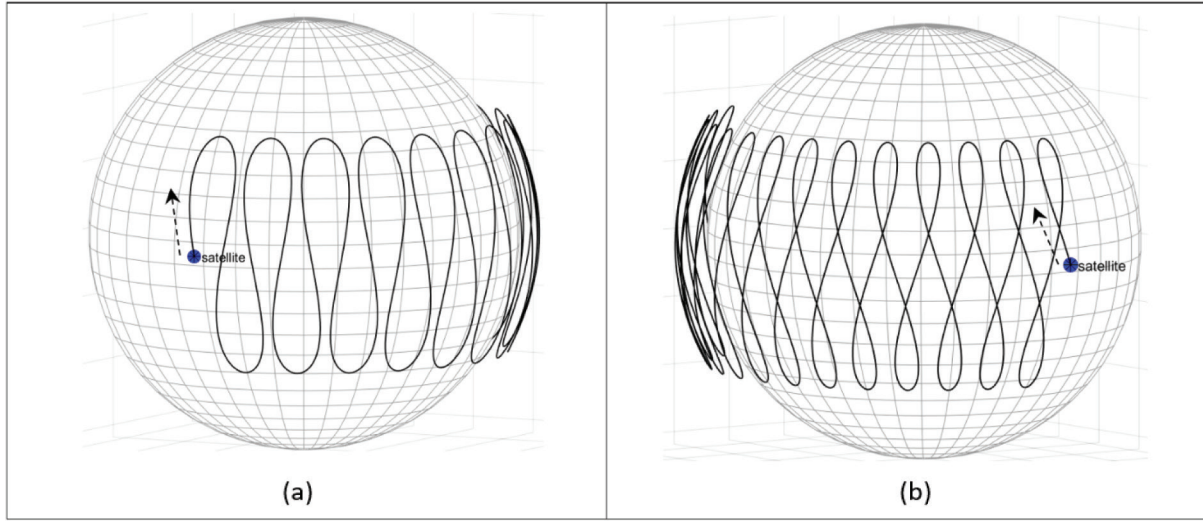


FIGURE 2 Hypocycloid and epicycloid motions near the GSO (a) Hypocycloid motion near GSO (b) Epicycloid motion near GSO

the satellite. This result indicates that if the rotation rates of the two objects are the same, the trajectory has a figure-eight shape and has characteristics identical to those of the GSO trajectory.

3 | SATELLITE PHASING RULE AND CLOSED-FORM SOLUTIONS

In this section, we aim to derive a satellite phasing rule for designing a GSO constellation with the purpose of having identical and non-identical constellation patterns. First, the identical constellation pattern design, in which all satellites in the constellation have the same ground track, is considered only for Ω and M_0 among the six orbital elements. For GSO satellites, the rotation rates of the Earth and the satellite are the same. This characteristic establishes the following relationship between Ω , the initial position of the Earth's rotation, and M_0 , the initial position of the satellite's rotation, for maintaining the same ground track:

$$M_0 = -\Omega \quad (8)$$

Therefore, the phasing rule for the same ground track of k GSO satellites can be arranged as follows:

$$\Omega_k = \Omega_1 + \theta_{\Omega_k} (k-1), \quad k = 1, 2, 3 \dots N \quad (9)$$

with:

$$M_{k0} = M_{10} - \Omega_k, \quad k = 1, 2, 3 \dots N \quad (10)$$

where θ_{Ω_k} is an interval of ascending node spacing.

For a GSO satellite constellation, which consists of the elliptical orbit from Equation (10), the argument of perigee, ω , for satellites with the same eccentricity is added to M_{k0} . The resulting phasing rule is as follows:

$$\Omega_k = \Omega_1 + \theta_{\Omega_k} (k-1), \quad k = 1, 2, 3 \dots N \quad (11a)$$

$$M_{k0} = M_{10} - (\Omega_k + \omega), \quad k = 1, 2, 3 \dots N \quad (11b)$$

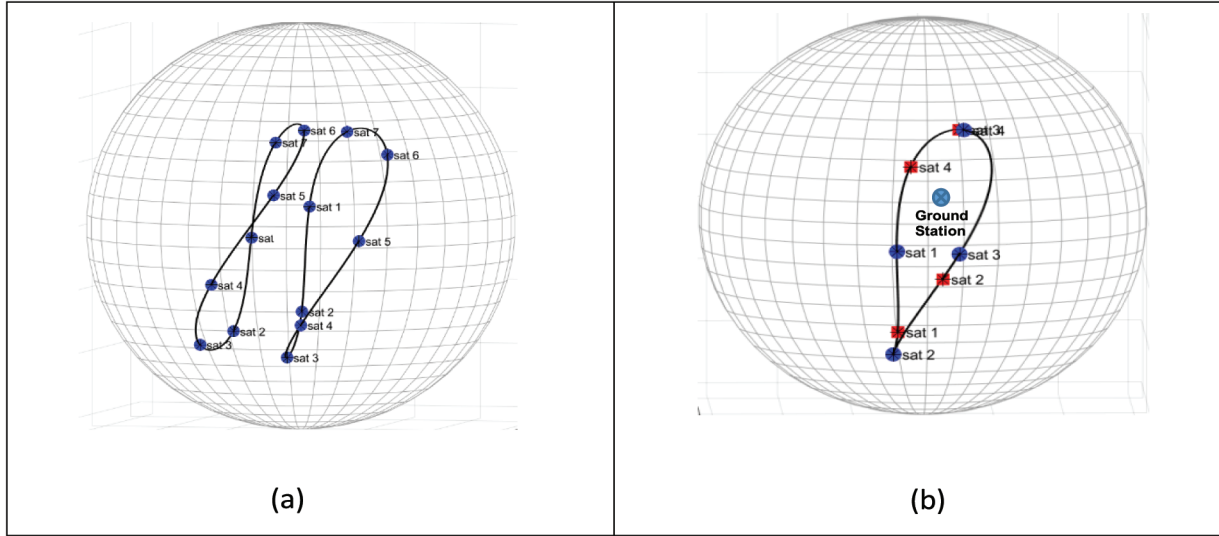


FIGURE 3 Change in GSO constellation according to ω and Ω values (a) Change in GSO ground track shape (b) Equally spaced (circles) and non-equally spaced (squares) placement

Next, a non-identical constellation pattern for GSO satellites is made possible by adding $\Delta\epsilon$ from the desired ground track interval and the initial mean anomaly. Thus, the phasing rule is given by the following:

$$M_{k0} = M_{10} - (\Omega_k + \omega) + \Delta\epsilon, \quad k = 1, 2, 3 \dots N \quad (12)$$

It is well known that the trajectory of a GSO satellite with an inclination has a figure-eight shape. Therefore, Equation (12) can place figure-eight shapes in non-identical patterns on the longitude in intervals of $\Delta\epsilon$ on the Earth's surface.

As a result, by substituting the phasing rule from Equation (11) into Equation (7), we obtain the following closed-form solution for which N_s satellites have the same GSO pattern:

$$x_k = \frac{r}{2} \left[(1 + \cos i) \cos(v_k - \omega_{\oplus} t + \omega + \Omega_k) + (1 - \cos i) \cos(v_k + \omega_{\oplus} t + \omega - \Omega_k) \right] \quad (13a)$$

$$y_k = \frac{r}{2} \left[(1 + \cos i) \sin(v_k - \omega_{\oplus} t + \omega + \Omega_k) - (1 - \cos i) \sin(v_k + \omega_{\oplus} t + \omega - \Omega_k) \right] \quad (13b)$$

$$z_k = r \sin i \sin(v_k + \omega) \quad (13c)$$

where $k = 1, 2, 3, \dots, N_s$ and the effect of the short-term perturbation by J_2 on the GSO is assumed to be small and is thus ignored. The closed-form solution in Equation (13) can directly describe the ground tracks of N_s satellites on the Earth's surface; in particular, it is observed that the three orbital elements Ω , M_0 , and ω play an important role in defining the GSO constellation configuration.

By evaluating the effect on the GSO ground track for each orbital element in Equation (13), it can be seen that the change in the shape of the GSO ground track is determined only by ω , the phase value of the z axis. Figure 3(a) shows the change in ground tracks as a function of ω values from 0° to 30° for seven GSO satellites with the same orbital elements. This change affects the relative dynamics between the ground station on the Earth's surface and the satellite, which is closely related to the performance (GDOP, navigation errors, etc.) of the satellite

TABLE 2

Comparison of GDOP Performance for Equally Spaced and Non-Equally Spaced Constellations

• $a = 42164.17$ km, $e = 0.1$, $i = 30^\circ$, $\omega = 45^\circ$ • Ground station: latitude = 10° , longitude = 27°		Mean GDOP
Equally spaced ($^\circ$)	<ul style="list-style-type: none"> • $\Omega_k = 0, 90, 180, 270$ • $M_{k0} = 315, 225, 135, 45$ 	67.938
Non-equally spaced ($^\circ$)	<ul style="list-style-type: none"> • $\Omega_k = 47.6, 165.9, 274.0, 317.3$ • $M_{k0} = 236.3, 160.8, 58, 6.6$ 	55.966

constellation. The next critical orbital element is Ω , which controls the satellite spacing of the GSO satellite constellation. In the case of GDOP, which generally measures GNSS performance, good results are obtained with equally spaced satellite placement. However, the performance of the satellite constellation varies depending on the location of the ground station and the spacing between satellites. Figure 3(b) shows equally spaced and non-equally spaced deployments for four satellites with $i = 30^\circ$ and $\omega = 45^\circ$, and the GDOP performance of the two satellite constellations is shown in Table 2. In some cases, the GDOP performance of the four satellites is better in non-equally spaced placements than in equally spaced placements for a specific ground station, as shown in Table 2. This result emphasizes that there are various GSO satellite constellation design cases, that evenly spaced constellations do not always have better performance than non-equally spaced constellations, and that better satellite constellation geometries can be found through simulations with the proposed solution. Thus far, no dedicated solution related to GSO satellite constellation design has been presented in the literature; accordingly, Equations (11)–(13) have academic novelty, providing a means to easily analyze various constellation designs and verify overall GDOP performance by simply substituting orbital elements into the closed-form solution.

4 | GDOP PERFORMANCE

This section examines the theoretical background for evaluating the performance of various GSO satellite constellations via the GDOP and the algorithm for applying the closed-form solution. The purpose of satellite navigation is to provide users with the time and actual position. However, the expected location and time differ from the user's actual position and time owing to various factors, including atmospheric errors and the geometry between the receiver and satellite. Navigation system errors can be broadly classified into two types. The first type is the statistical user equivalent range error (UERE) that occurs during the distance measurement process. The second error type is the GDOP error caused by the geometric arrangement of the navigation satellites. The GDOP reduces the accuracy of the time and position calculated at the receiver end. In contrast, the UERE includes errors due to satellites, receiver clock biases, atmospheric propagation, and multipaths. Here, errors caused by the geometric characteristics of the satellite receiver can be minimized by maintaining a good geometric arrangement between the satellite and the user (Sharp et al., 2009; Langley, 1999; El-Hakim, 2023).

The GDOP can be used to determine how to deploy satellites to provide accurate positioning and time services to users. Figure 4 shows a flowchart

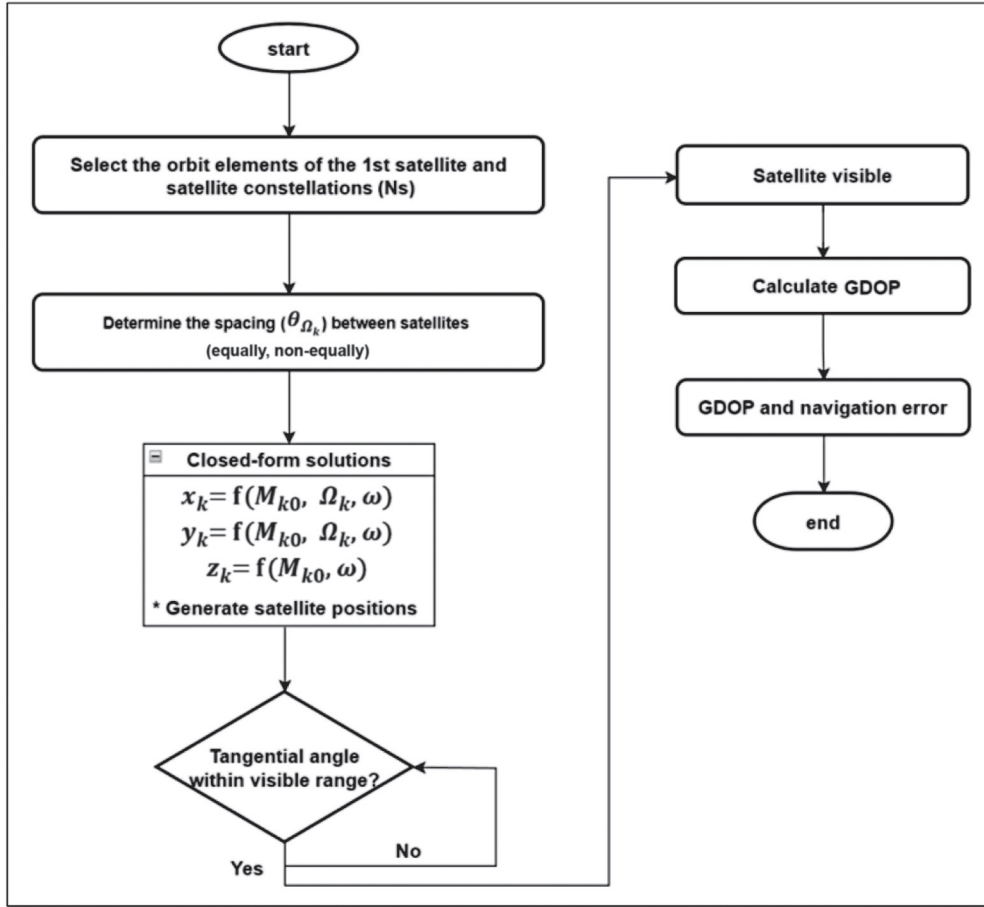


FIGURE 4 Implementation of the GDOP performance algorithm for assessing a satellite constellation via the application of a closed-form solution

for obtaining the GDOP performance for various constellation configurations by applying the closed-form solution proposed in this study. First, the orbital elements of the first satellite are set and the total number of satellites (N_s) is determined. The GDOP performance for a specific ground station is calculated based on considerations such as the location of the ground station and the spacing (θ_{Ω_k}) between satellites. Under the same orbital element conditions, the closed-form solution simply calculates the position of each satellite distributed by the phasing rule of Ω_k and M_{k0} while minimizing the computational load. Here, we examine the steps for calculating the GDOP and obtain the unit vector for the position vector between the satellite and desired receiver using Equation (13):

$$\left(\frac{x_k - x}{\rho_k}, \frac{y_k - y}{\rho_k}, \frac{z_k - z}{\rho_k} \right) \quad (14)$$

where:

$$\rho_k = \sqrt{(x_k - x)^2 + (y_k - y)^2 + (z_k - z)^2} \quad (15)$$

In Equation (15), $x, y,$ and z are the ECEF coordinates of the user receiver, and $x_k, y_k,$ and z_k are the ECEF coordinates of the k -th satellite. Matrix A for the pseudorange measurement residual equations is formulated as follows:

$$\begin{pmatrix} \frac{x_1 - x}{\rho_1} & \frac{y_1 - y}{\rho_1} & \frac{z_1 - z}{\rho_1} & -1 \\ \frac{x_2 - x}{\rho_2} & \frac{y_2 - y}{\rho_2} & \frac{z_2 - z}{\rho_2} & -1 \\ \frac{x_3 - x}{\rho_3} & \frac{y_3 - y}{\rho_3} & \frac{z_3 - z}{\rho_3} & -1 \\ \vdots & \vdots & \vdots & \vdots \end{pmatrix} \quad (16)$$

If the element in the fourth column of matrix A is -1 , the time dilation of precision (TDOP) is calculated appropriately. Based on matrix A , the covariance matrix Q can be obtained, which is used to determine the GDOP, position dilation of precision (PDOP), and TDOP as follows:

$$Q = (A^T A)^{-1} \quad (17)$$

and:

$$\begin{pmatrix} \sigma_x^2 & \sigma_{xy} & \sigma_{xz} & \sigma_{xt} \\ \sigma_{xy} & \sigma_y^2 & \sigma_{yz} & \sigma_{yt} \\ \sigma_{xz} & \sigma_{yz} & \sigma_z^2 & \sigma_{zt} \\ \sigma_{xt} & \sigma_{yt} & \sigma_{zt} & \sigma_t^2 \end{pmatrix} \quad (18)$$

PDOP, TDOP, and GDOP are given as follows:

$$PDOP = \sqrt{\sigma_x^2 + \sigma_y^2 + \sigma_z^2} \quad (19)$$

$$TDOP = \sqrt{\sigma_t^2} \quad (20)$$

$$GDOP = \sqrt{\text{tr } Q} \quad (21)$$

The GDOP represents the comprehensive uncertainty of time and position due to the satellite constellation geometry and is used to determine the performance index of the space segment design of the satellite system. If the GDOP value is small, the uncertainty of the user's position is also small. The GDOP value changes as the satellite position changes with respect to the ground location. Therefore, the overall mean value of the GDOP can be used as a measure of constellation performance.

5 | SIMULATION RESULTS

In the previous section, a closed-form solution and satellite phasing rules for designing a ground track and satellite constellation were proposed based on the geometric principles of Ptolemaic deferent-epicycle and spring-mass systems. In this section, the point and regional coverage obtained for different GDOP values are evaluated to analyze the performance of GSO constellations.

5.1 | Point Coverage

We analyzed the performance of two satellite constellation patterns using the analytical solution and phasing rules presented above. A performance analysis was performed by comparing the GDOP values. The GSO constellations were designed such that seven satellites ($k = 7$) have identical ground tracks, according to Equation (13). Table 3 lists the specifications of the two types of GSO constellations, which have different eccentricities/arguments of perigee. The spacing of the ascending nodes is 51.4° .

As shown in Figure 5, the GSO I constellation has seven satellites evenly distributed in a circular orbit and a symmetrical structure with a ground station on the equator. The GDOP values present sinusoidal curve characteristics. The GSO II constellation shown in Figure 6 has an eccentricity of 0.1 and an argument of perigee of 90° . Therefore, the figure-eight-shaped crossing point descends toward the south. The distribution of GDOP values exhibits an irregular curve for the equatorial ground station. However, the mean GDOP values of the two GSO constellations were 2–4 for a ground station located at the equator, indicating excellent performance.

5.2 | Regional Coverage

This section compares the performance of regional GDOP values as the ground station location is varied, aiming to analyze the local coverage for various GSO constellation patterns. The GSO constellation patterns are divided into identical patterns, in which all satellites have the same ground track, and non-identical patterns, in which the satellites have different ground tracks. In this study, for

TABLE 3
Specifications for Two Types of GSO Constellations

	a	e	i	ω	Ω_k
GSO I	42164.17km	0.0	60°	0°	$\theta_{\Omega_k} = 51.4^\circ$
GSO II	42164.17km	0.1	60°	90°	

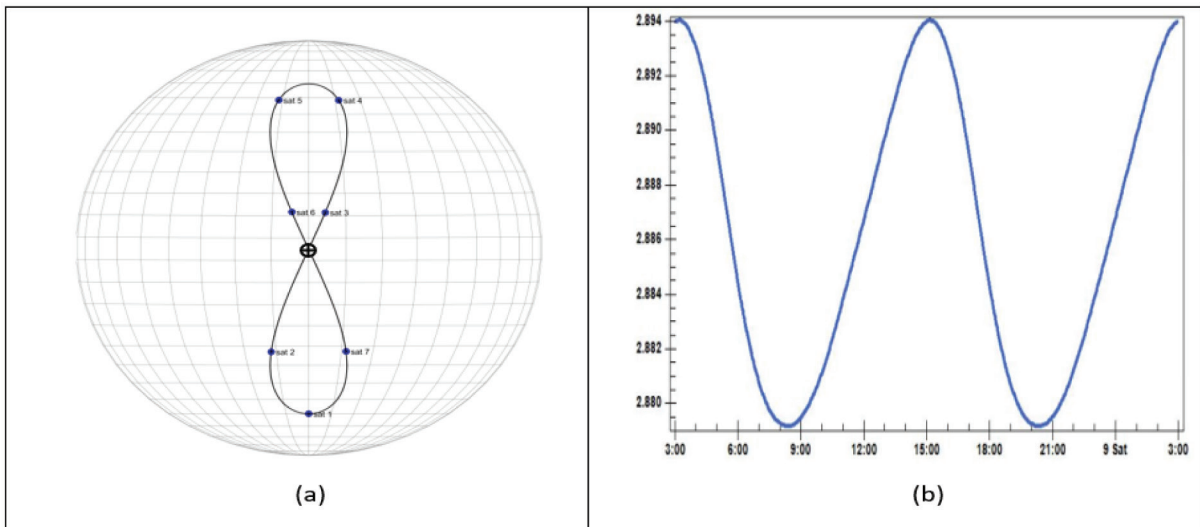


FIGURE 5 Constellation and GDOP performance for a circular GSO (a) Circular GSO I pattern (b) Time vs. GDOP values

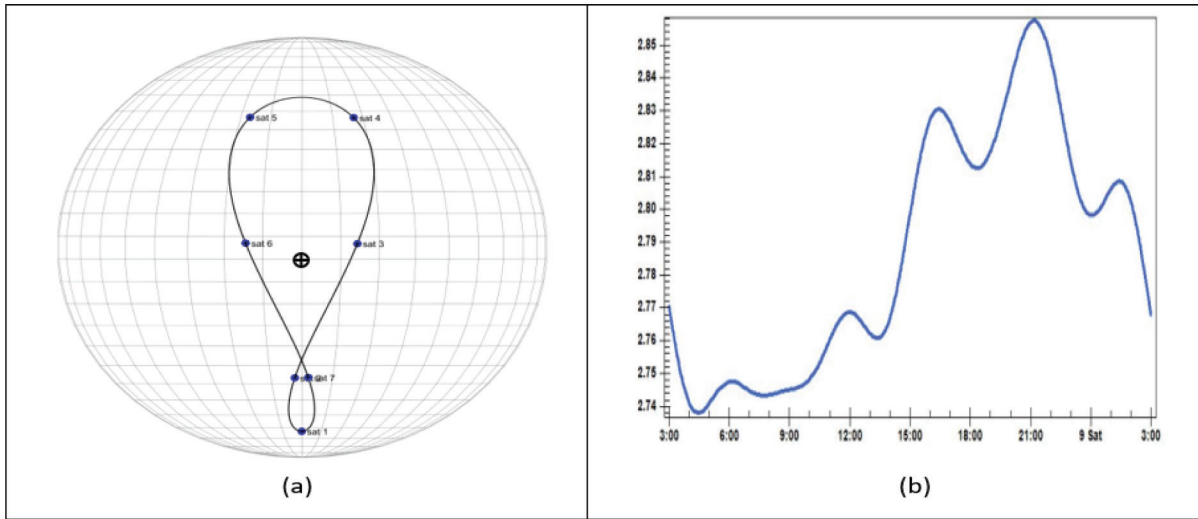


FIGURE 6 Constellation and GDOP performance for a noncircular GSO (a) Noncircular GSO II pattern (b) Time vs. GDOP values

TABLE 4
Specifications for Two Types of GSO Constellations

	a	e	i	ω	Ω_k	M_{k0}
Case I	42164.17 km	0.0	60°	0°	$\theta_{\Omega_k} = 51.4^\circ$	$\Delta\epsilon = 0^\circ$
Case II	42164.17 km	0.1	60°	90°		$\Delta\epsilon = \pm 20^\circ$

convenience, the number of satellites in an identical pattern is denoted as σ_i , and the number of satellites in a non-identical pattern is denoted as σ_n . For the regional coverage analysis, we determined the GDOP value while constantly changing the ground station latitude based on the longitude of the GSO crossing point.

Two types of GSO constellations with seven satellites were compared and analyzed for the case of $\sigma_i = 7/\sigma_n = 0$, which consists of only identical patterns, and $\sigma_i = 3 \times 2/\sigma_n = 1$, which consists of two patterns combined. Table 4 presents the specifications of the satellite constellations used for the comparative analysis.

Figure 7 presents the results for case I, as described in Table 4, with an identical circular GSO constellation. The circularly identical GSO pattern shown in Figure 7(a) implies that the GDOP values of the symmetrically distributed ground stations are symmetric about the equator. The best GDOP value is observed for the location at the equator; as the distance from the equator increases, the GDOP performance becomes worse. Figure 7(b) illustrates three GSO patterns, with the figure-eight in the middle being the trajectory of one satellite and the figure-eights on both sides consisting of three satellites. Compared with the results shown in Figure 7(a), the GDOP performance is improved at the Equator, but the overall deviation from the ground station is notably large. This result indicates that, in the case of a circular GSO, maintaining an identical constellation pattern for all satellites helps improve the GDOP performance.

Figure 8 presents the results for case II, as described in Table 4, with a non-identical GSO constellation. For the non-identical pattern in Figure 8(a), the crossing point of the figure-eight moves to the southern hemisphere owing to the eccentricity and the argument of perigee. The variation in GDOP values is markedly large, especially in the northern hemisphere, where there are no crossing points, and the GDOP performance is very poor. Figure 8(b) displays a constellation with combined patterns of a GSO in an elliptic orbit. Although the GDOP

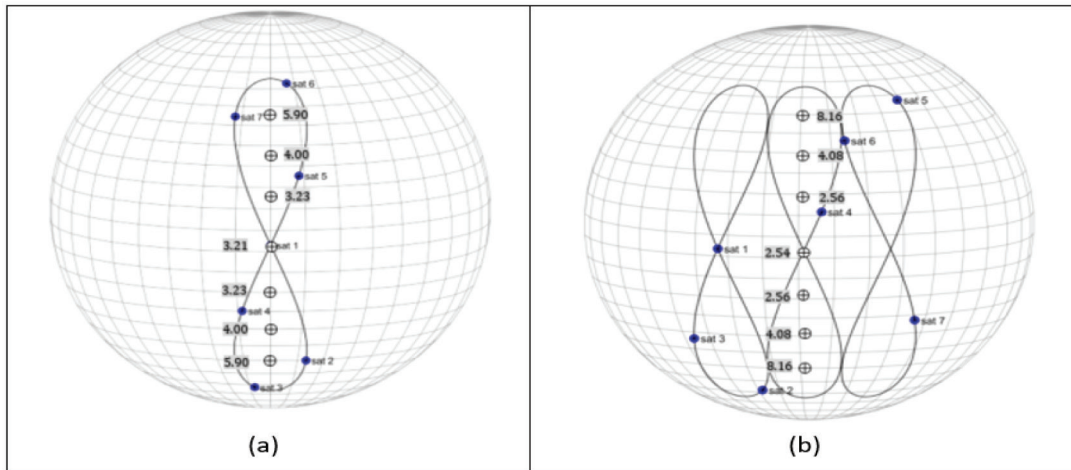


FIGURE 7 Regional GDOP distribution for a circular pattern (a) Only circular orbit pattern (b) Combined circular orbit pattern

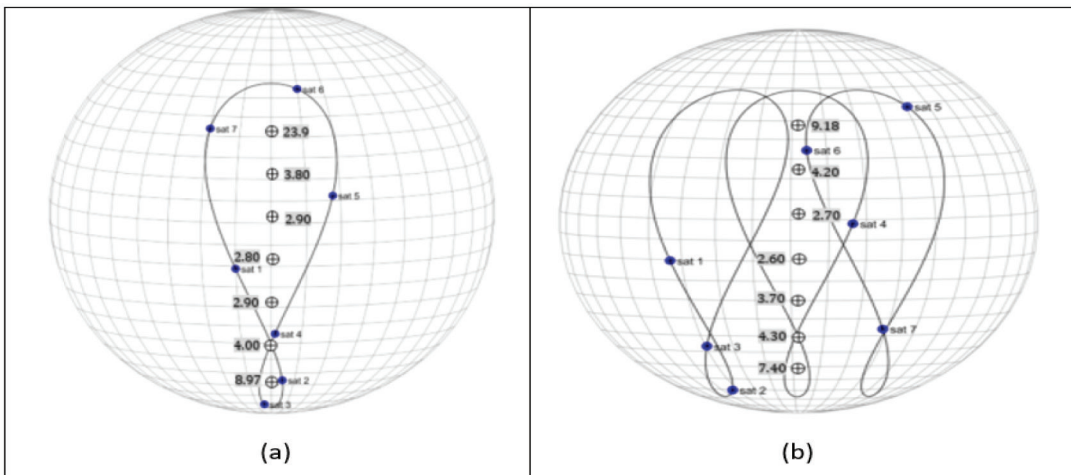


FIGURE 8 Constellation and GDOP performance for a noncircular GSO (a) Only elliptical orbit pattern (b) Combined elliptical orbit pattern

performance is marginally better than that shown in Figure 8(a), it is still worse than that of the circular pattern. The QZSS and KPS are representative examples that leverage a noncircular orbit pattern. For the constellation patterns of these navigation satellite systems, engineers can improve the performance of the GDOP by moving the crossing point of the elliptical orbit toward the region of each respective country in the northern hemisphere.

Figure 9 presents the results from Figures 7 and 8 according to the latitude of the ground station. Overall, for latitudes from -30° to 30° , the GDOP value remains at 4 or less, showing excellent performance. For all constellation patterns, the ground station at the equator exhibits the best GDOP performance. In summary, the identical circular pattern is stable and exhibits the best performance in regional areas compared with other patterns. Even for circular orbits, the GDOP performance gap between the northern and southern hemispheres widens as it shifts toward a non-identical pattern. In addition, the elliptical orbit pattern moves the crossing point of the figure-eight to the southern or northern hemisphere, depending on the value of the argument of perigee, which causes the GDOP performance to be biased toward one region.

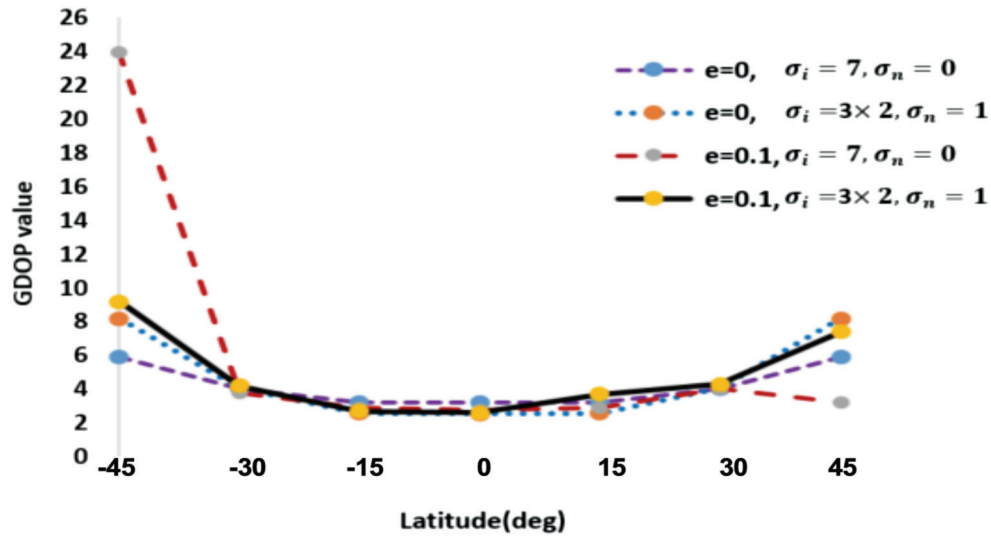


FIGURE 9 Regional GDOP values as a function of the ground station latitude

6 | CONCLUSIONS

The dedicated tool proposed in this study worked effectively and obtained meaningful results for analyzing and evaluating the GDOP performance of point and regional coverage of various GSO satellite constellations. Specifically, the point coverage was used to compare the GDOP performance of circular and noncircular GSO patterns for seven evenly distributed satellites. Here, the GDOP performance exhibited average GDOP values of 2–4 for ground stations located at the equator, irrespective of the GSO constellation. To evaluate the regional coverage performance, the regional GDOP distribution was analyzed for various GSO patterns. The ground station located on the equator displayed the best GDOP performance. Moreover, for a satellite group with a given number of satellites, the ideal constellation pattern showed better performance than that with multiple ground track patterns. Additionally, the crossing point location on the figure-eight trajectory contributes to the improved GDOP performance. The ideal crossing point location should correspond to a ground station location at any point on the equator.

DATA AVAILABILITY

The authors declare that all data relevant to this study are available within the paper.

ACKNOWLEDGMENTS

This work was supported by the Institute of Information & Communications Technology Planning & Evaluation (IITP) grant funded by the Korean government (MSIT) (No. 1711195701, Development of metaverse-based space object orbital information visualization and linkage technology).

DECLARATION OF COMPETING INTERESTS

None.

REFERENCES

- Bai, S., Zhang, Y., Jiang, Y., Sun, W., & Shao, W. (2024). Modified two-dimensional coverage analysis method considering various perturbations. *IEEE Transactions on Aerospace and Electronic Systems*, 60(3), 2763–2777. <https://doi.org/10.1109/TAES.2023.3348423>
- Bandemer, B., Denks, H., Hornbostel, A., & Konovaltsev, A. (2006). Performance of acquisition methods for Galileo SW receivers. *European Journal of Navigation*, 4(3), 17–19. <https://elib.dlr.de/19799/>
- El-Hakim, H. A., & Mohamed, H. A. (2023). Engineering planar antenna using geometry arrangements for wireless communications and satellite applications. *Scientific Reports*, 13, 19196. <https://doi.org/10.1038/s41598-023-46400-9>
- Gu, Y., Chen, Y., Zhang, Y., Wu, G., & Bai, S. (2024). Extended 2-D map for satellite coverage analysis considering elevation-angle constraint. *IEEE Transactions on Aerospace and Electronic Systems*, 60(5), 6531–6549. <https://doi.org/10.1109/TAES.2024.3409681>
- JAXA QZSS Project Team (2009). Current status of Quasi-Zenith Satellite System. *Proc. of the 2009 4th International Committee on GNSS*, 14–18. <https://www.unoosa.org/documents/pdf/icg/activities/2009/icg4/05-1.pdf>
- Karutin, S. (2020). The status of GLONASS system. *Proc. of the 33rd International Technical Meeting of the Satellite Division of the Institute of Navigation (ION GNSS+)*, 21–25. <https://doi.org/10.33012/2020.17553>
- Kim, T. (2019). Status of KPS plans-Korea Positioning System. *Proc. of the Fourteenth Meeting of the International Committee on Global Navigation Satellite Systems (ICG), Bengaluru, India*. <https://www.unoosa.org/documents/pdf/icg/2019/icg14/14.pdf>
- Kuiack, B., & Ulrich, S. (2018). Nonlinear analytical equations of relative motion on J_2 -perturbed eccentric orbits. *Journal of Guidance, Control, and Dynamics*, 41(12), 2664–2674. <https://doi.org/10.2514/1.G003723>
- Langley, R. B. (1999). Dilution of precision. *GPS World*, 10(5), 52–59. <https://www.gpsworld.com/gnss-systemalgorithms-methodsinnovation-improving-dilution-precision-9100/>
- Lee, S. S., & Hall, C. D. (2021). Parametric approach for satellite relative orbit designs and constellations. *Journal of Guidance, Control, and Dynamics*, 44, 488–492. <https://doi.org/10.2514/1.G005440>
- Mukesh, R., Karthikeyan, V., Soma, P., Sindhu, P., & Elangovan, R. R. (2020). Performance analysis of navigation with Indian constellation satellites. *Journal of King Saud University, Engineering Sciences*, 32(8), 518–523. <https://doi.org/10.1016/j.jksues.2019.06.002>
- Noer, A., Armin, F., & Wejay, J. A. C. (2020). Design of optimal satellite constellation for Indonesian regional navigation system based on GEO and GSO satellites. *Proc. of the 2020 3rd International Seminar on Research of Information Technology and Intelligent System (ISRITI), Yogyakarta, Indonesia*, 289–294. <https://doi.org/10.1109/ISRITI51436.2020.9315405>
- Sharp, I., Yu, K., & Guo, Y. J. (2009). GDOP analysis for positioning system design. *IEEE Transactions on Vehicular Technology*, 58(7), 3371–3382. <https://doi.org/10.1109/TVT.2009.2017270>
- Shen, J., & Geng, C., (2020). Updated on the BeiDou Navigation Satellite System (BDS). *Proc. of the 33rd International Technical Meeting of the Satellite Division of the Institute of Navigation (ION GNSS+ 2020)*, 978–1015. <https://doi.org/10.33012/2020.17555>
- Shin, M., Kim, D. W., Chun, S., & Heo, M. B. (2019). A study on the satellite orbit design for KPS requirements. *Journal of Positioning, Navigation, and Timing*, 8(4), 215–223. <https://doi.org/10.11003/JPNT.2019.8.4.215>
- Sjoberg, L. E., Grafarend, E. W., & Joud, M. S. S. (2017). The zero gravity curve and surface and radii for geostationary and geosynchronous satellite orbits. *Journal of Geodetic Science*, 7, 43–50. <https://doi.org/10.1515/jogs-2017-0005>
- Ye, H., JunJing, X., Liu, L., Wang, M., Hao, S., Lang, X., & Yu, B. (2020). Analysis of Quasi-Zenith Satellite System signal acquisition and multiplexing characteristics in China area. *Sensors*, 20, 1547. <https://doi.org/10.3390/s20061547>

How to cite this article: Lee, S. S. (2025). Analytical solution and satellite phasing rules for designing dedicated geosynchronous orbit satellite constellations. *NAVIGATION*, 72(3). <https://doi.org/10.33012/navi.711>